



www.sciencemag.org/cgi/content/full/1167093/DC1

Supporting Online Material for

Optical Deconstruction of Parkinsonian Neural Circuitry

Viviana Gradinaru, Murtaza Mogri, Kimberly R. Thompson, Jaimie M. Henderson,
Karl Deisseroth*

To whom correspondence should be addressed. E-mail: deissero@stanford.edu

Published 19 March 2009 on *Science Express*
DOI: 10.1126/science.1167093

This PDF file includes

Materials and Methods
Figs. S1 to S7
Table S1
References

Optical Deconstruction of Parkinsonian Neural Circuitry

Supporting online material

MATERIALS AND METHODS

Immunohistochemistry and imaging

To verify the phenotype of cells and measure c-fos activity, rodents were anaesthetized with 65 mg/kg sodium pentobarbital and transcardially perfused with ice-cold 4% paraformaldehyde (PFA) in PBS (pH 7.4). Brains were fixed overnight in 4% PFA and then equilibrated in 30% sucrose in PBS. 40 μm -thick coronal sections were cut on a freezing microtome and stored in cryoprotectant at 4°C until processed for immunohistochemistry. Free-floating sections were washed in PBS and then incubated for 30 min in 0.3% Triton X-100 (Tx100) and 3% normal donkey serum (NDS). Slices were incubated overnight with primary antibody in 0.01% Tx100 and 3% NDS (rabbit anti-cfos 1:500, rabbit anti-GFAP 1:500, mouse anti-MAP2 1:500, mouse anti-GAD67 1:500, rabbit anti-GABA 1:200, mouse anti-vGlut1 1:500, mouse anti-vGlut2 1:500, mouse anti-CaMKII α 1:200, mouse anti-S100 β 1:250, rabbit anti-glutamate 1:200, chicken anti-tyrosine hydroxylase 1:500, and goat anti-choline acetyltransferase 1:200). Sections were then washed and incubated with secondary antibodies (1:1000) conjugated to FITC, Cy3 or Cy5 for 3 hrs at room temperature. Following a 20 min incubation with DAPI (1:50,000) sections were washed and mounted on microscope slides with PVA-DABCO.

Confocal fluorescence images were acquired on a scanning laser microscope using a 20X/0.70NA or a 40X/1.25NA oil immersion objective. To determine the volume of c-fos activation, serial stack images covering a depth of 20 μm through multiple medial-lateral, anterior-posterior and dorsal-ventral subthalamic sections were acquired using equivalent settings. The image analysis software calculated the number of c-fos positive cells per field by thresholding c-fos immunoreactivity above background levels and using the DAPI staining to delineate nuclei. To determine the rate of viral transduction we determined the percentage of CaMKII α -immunoreactive neurons per 40X field that were also eNpHR-YFP positive in

multiple serial stack images of subthalamic sections. Large field images of entire slices were collected on a Leica MZ16FA stereomicroscope.

Lentivirus production and transduction

Lentiviral vectors carrying the genes used were constructed using standard cloning techniques. The CaMKII α ::eNpHR construct was produced by PCR amplification of the eNpHR-EYFP construct previously published (S1) and cloned in-frame into the AgeI and EcoRI restriction sites of a lentivirus carrying the CaMKII α promoter. The CaMKII α ::ChR2 construct was produced by PCR amplification of the ChR2-mCherry construct and was also cloned in-frame into the AgeI and EcoRI restriction sites of a lentivirus carrying the CaMKII α promoter. The GFAP::ChR2 construct was produced by replacing the CaMKII α promoter with the GFAP promoter in the CaMKII α ::ChR2-mCherry construct using the AgeI and PacI restriction enzyme sites. The maps for CaMKII α ::ChR2 and CaMKII α ::eNpHR are available online at www.optogenetics.org.

High titer lentivirus ($>10^9$ pfu/mL) was then produced via calcium phosphate co-transfection of 293FT cells with the lentiviral vector, pCMV Δ R8.74 and pMD2.G (S2). 24 h post-transfection, 293FT cells were switched to serum-free medium containing 5 mM sodium butyrate; the supernatant was collected 16 h later and concentrated by ultracentrifugation at $50,000 \times g$ with 20% sucrose cushion. The resulting viral pellet was resuspended in phosphate buffered saline at 1/1000th of the original volume.

Adeno-associated virus production and transduction

To ensure that there would be no significant expression leak in non-targeted cell types, we employed a Cre-inducible AAV vector with a double-floxed inverted open reading frame (ORF), wherein the ChR2-EYFP sequence is present in the antisense orientation. Upon transduction, Cre-expressing cells invert the ChR2-EYFP ORF in a stable, irreversible fashion and thereby activate sustained ChR2-EYFP expression under control of the strong and constitutively active elongation factor 1 α (EF-1 α) promoter (Feng Zhang, unpublished results). To construct Cre-activated recombinant AAV vectors, the DNA cassette carrying two pairs of incompatible lox sites (loxP and lox2722) was synthesized and the ChR2-EYFP transgene was inserted between

the loxP and lox2722 sites in the reverse orientation. The resulting double-floxed reverse ChR2-EYFP cassette was cloned into a modified version of the pAAV2-MCS vector carrying the EF-1 α promoter and the Woodchuck hepatitis virus posttranscriptional regulatory element (WPRE) to enhance expression. The recombinant AAV vectors were serotyped with AAV5 coat proteins and packaged by the viral vector core at the University of North Carolina. The final viral concentration was 2×10^{12} genome copies (gc) / mL.

Stereotactic injection and cannula placement

Adult rats (female Fisher, 200–300 g) and mice (male and female, C57BL/6 background, 15–30 g) were the subjects of these experiments. Animal husbandry and all aspects of experimental manipulation of our animals were in strict accord with guidelines from the National Institute of Health and have been approved by members of the Stanford Institutional Animal Care and Use Committee. All surgeries were performed under aseptic conditions. Rodents were anaesthetized using 1.5% isoflurane (for surgeries longer than 1 hr) or i.p. injection (90 mg/kg ketamine and 5mg/kg xylazine for rats; 80 mg/kg and 15-20 mg/kg, respectively, for mice). The top of the animal's head was shaved, cleaned with 70% ethanol and betadine and then placed in a stereotactic apparatus. Ophthalmic ointment was applied to prevent eye drying. A midline scalp incision was made and then small craniotomies were performed using a drill mounted on the stereotactic apparatus for the 6-OHDA injection in the medial forebrain bundle (rat: -2 AP, 2 ML, -7.5 DV; mouse: -1.2 AP, 1.2 ML, -4.75 DV) and virus injection in the STN (rat: -3.6 mm AP, 2.5 mm ML; mouse: -1.9 mm AP, 1.7 mm ML).

For rodents that were injected with lentivirus in the STN, *in vivo* extracellular recording was used to accurately determine the location of the STN along the dorsal-ventral axis. The depth was around -7 mm in rats and -4 mm in mice. The concentrated lentivirus (described above) was delivered to the STN using a 10 μ l syringe and a thin 34 gauge metal needle; the injection volume and flow rate (3 sites within the STN along the dorsal-ventral axis; each injection was 0.6 μ l at 0.1 μ l/min) was controlled with an injection pump. After the final injection, the needle was left in place for 10 additional minutes and then slowly withdrawn.

6-OHDA was then used to lesion the substantia nigra and produce hemi-Parkinsonian rodents. Desipramine (20mg/kg for rats; 10 mg/kg for mice; noradrenergic reuptake inhibitor to prevent damage to noradrenergic terminals) was administered, followed ~30 minutes later by 6-OHDA (8 µg/4 µl for rats; 6 µg/2 µl for mice) with 0.1% ascorbic acid (to prevent degradation of 6-OHDA) into the right medial forebrain bundle (rat: -2 AP, +2 ML, and -7.5 DV; mouse: -1.2 AP, +1.2 ML, and -4.75 DV). The perfusion for the 6-OHDA injection (rat: 4 µl, mouse 2 µl) was at the rate of 1.2 µl/min for 4 min, and the needle was left *in situ* for an additional 5 minutes.

A fiber guide (rat: C312G, mouse: C313G) was beveled to form a sharp edge (to more easily penetrate brain tissue and reduce tissue movement), and then inserted through the craniotomy to a depth of approximately 400 µm above the STN or the anterior primary motor cortex (mouse: 2 AP, 2 ML, 0.5 DV). One layer of adhesive cement followed by cranioplastic cement was used to secure the fiber guide system to the skull. After 20 min, the scalp was sealed back using tissue adhesive. The animal was kept on a heating pad until it recovered from anesthesia. Buprenorphine (0.03 mg/kg) was given subcutaneously following the surgical procedure to minimize discomfort. A dummy cannula (rat: C312G, mouse: C313G) was inserted to keep the fiber guide patent.

For electrical DBS control rodents, a stimulation electrode (MS303/3-B) was implanted in the STN. The procedure above was followed for OHDA injection, *in vivo* extracellular recording was then used to determine the depth of the STN, and the stimulation electrode was inserted to that depth and secured using one layer of adhesive cement followed by cranioplastic cement. Tissue adhesive was used to reseal the scalp, the animal was kept on a heating pad until recovery from anesthesia and buprenorphine was given to minimize discomfort. A dust cap (303DC/1) was then used to cover the electrode contacts.

In vivo optrode recordings

Simultaneous optical stimulation and electrical recording in a single region in living rodents was done as described previously (S3) using an optrode composed of an extracellular tungsten electrode (1 MΩ, ~125 µm) tightly attached to an optical fiber (~200 µm) with the tip of the

electrode deeper (~0.4 mm) than the tip of the fiber, to ensure illumination of the recorded neurons. For stimulation and recording in two distinct regions, small craniotomies were created above both target regions, and a fiber or optrode was placed above one region through one craniotomy and a plain electrode or optrode was placed in the other region through a separate craniotomy (see Fig. 6B for diagram; the picture is modified from The Jackson Laboratory website: http://jaxmice.jax.org/support/Thy1-ChR2-9_WholeBrain4x.pdf). Stimulation in the anterior motor cortex was achieved by placing the optical fiber just above the brain surface, activating layer 5 of the cortex; for STN stimulation, the fiber was 300 μm above the STN. The STN was identified using its highly stereotyped firing pattern and the fact that it is surrounded dorso-ventrally by silent regions. The optical fiber was coupled to a 473 nm or 561 nm laser diode (30 mW fiber output) from CrystaLaser. Single unit recordings were done in rats anesthetized with 1.5% isoflurane and mice anesthetized with intraperitoneal injections of ketamine (80 mg/kg)/xylazine (15-20 mg/kg) cocktail. pClamp 10 and a Digidata 1322A board were used to both collect data and generate light pulses through the fiber. The recorded signal was band pass filtered at 300Hz low/5 kHz high (1800 Microelectrode AC Amplifier). For precise placement of the fiber/electrode pair, stereotactic instrumentation was used.

Behavior

For behavior, multimode optical fibers (NA 0.37; rat: 400 μm core, BFL37-400; mouse: 300 μm core, BFL37-300) were precisely cut to the optimal length for maximizing the volume of the STN receiving light. About one week before behavior, an extracellular recording electrode was used to determine the depth of the dorsal border of the STN from the tip of the cannula guide and fibers were cut to be 200-300 μm shorter. For anterior motor cortex stimulation, the fiber was placed above layer 5 (less than a millimeter deep). To ensure stability of the fiber during testing in moving animals, an internal cannula adapter was glued to the stripped optical fiber. To insert the fiber, rodents were briefly placed under isoflurane and the fiber was inserted while the animal was recovering from anesthesia. The internal cannula adapter snapped onto the cannula guide and the bottom half of the plastic portion of a dummy cannula was also used to ensure the adapter remained connected to the top of the cannula guide (S3, S4).

For optical stimulation, the fiber was connected to a 473 nm or 561 nm laser diode (20 mW fiber output) through an FC/PC adapter. Laser output was controlled using a function generator (33220A) to vary the frequency, duty cycle, and intensity. For Thy1::ChR2 animals, the average minimum intensity used to produce therapeutic behavior was 10 mW. A custom aluminum rotating optical commutator (S3, S4) was used to release torsion in the fiber caused by the animal's rotation.

Motor behavior was assessed using amphetamine-induced rotations, head position bias, climbing, and track length. Animals were accepted for experimental investigation only if amphetamine reliably induced rotations in the ipsilateral direction confirming a 6-OHDA lesion of the substantia nigra. Before and after each stimulation trial, a trial of equal length with the light off was used as a control. Each of these trials was about 3 minutes long making the entire off-on-off sequence 9 minutes long. For amphetamine-induced behavior, amphetamine (rat: 2 mg/kg; mouse: 2.6 mg/kg) was injected 30 minutes before behavioral measurements; the fiber was inserted into the cannula and the rodent placed in an opaque, non-reflective cylinder (rat: diameter 25 cm, height 61 cm; mouse: diameter 20 cm, height 46 cm) 10 minutes before the behavioral experiments. Rotations ipsilateral to the 6-OHDA lesions (clockwise turns) were counted, and contralateral rotations were subtracted. The percentage change calculation considered the change in rotational bias relative to the period without stimulation. Head position bias was determined by counting the number of head tilts ($>10^\circ$ deviation left or right of midline) over time. Each time the rodent rose up and touched either paw to the wall of the cylinder was counted as an instance of climbing. Track length was measured with Viewer. After the completion of behavior experiments, cannula placement was confirmed by slicing.

For experiments where optical stimulation did not produce a change in the rodent behavior, we also collected path length and head position bias data while the rodents were under amphetamine. Continuous 561nm illumination of the STN expressing CaMKII α ::eNpHR-EYFP in 6-OHDA rats did not affect path length (cm/min; light on vs. light off: 757.05 ± 163.11 vs. 785.74 ± 157.56 , $p = 0.90$, $n = 4$ rats; mean \pm s.e.m; 2-sample t -test) or head position bias (% of time to the right; light on vs. light off: 99.92 ± 0.08 vs. 99.75 ± 0.25 , $p = 0.56$, $n = 4$ rats; mean \pm

s.e.m; 2-sample *t*-test). Optical HFS (120 Hz, 5 ms pulse width) or LFS (20 Hz, 5 ms pulse width) of the STN expressing CaMKII α ::ChR2-mCherry in 6-OHDA rats did not affect path length (cm/min; HFS vs. light off: 803.82 ± 129.04 vs. 851.95 ± 166.20 , $p = 0.83$, $n = 5$ rats; LFS vs. light off: 847.15 ± 141.95 vs. 779.11 ± 104.01 , $p = 0.74$, $n = 2$ rats; mean \pm s.e.m; 2-sample *t*-test) or head position bias (% of time to the right; HFS vs. light off: 93.97 ± 3.78 vs. 94.20 ± 2.96 , $p = 0.96$, $n = 5$ rats; LFS vs. light off: 98.50 ± 1.50 vs. 98.50 ± 0.50 , $p = 1.00$, $n = 2$ rats; mean \pm s.e.m; 2-sample *t*-test). 473nm illumination of the STN expressing GFAP::ChR2-mCherry in 6-OHDA rats also did not affect path length (cm/min; light on vs. light off: 1042.52 ± 113.73 vs. 1025.47 ± 113.63 , $p = 0.92$, $n = 4$ rats; mean \pm s.e.m; 2-sample *t*-test) or head position bias (% of time to the right; light on vs. light off: 98.16 ± 0.98 vs. 98.98 ± 0.65 , $p = 0.52$, $n = 4$ rats; mean \pm s.e.m; 2-sample *t*-test).

Optical Intensity Measurements

Light transmission measurements were conducted with blocks of brain tissue prepared from two 300 g Fisher rats and immediately tested. Blocks of tissue 2 mm in thickness were cut in 0–4 °C sucrose solution using a vibratome. The tissue was then placed in a Petri dish containing the same sucrose solution over the photodetector of a power meter. The tip of a 200 μ m diameter optical fiber coupled to a blue or yellow diode laser (473 nm or 561 nm, 30 mW fiber output) was mounted on a micromanipulator. First, the power was measured through the solution. Then, the tip of the fiber was moved down into the tissue in 100 μ m increments and the power was measured. When the fiber reached the Petri dish, the power measured was compared to the initial measurement through the solution to confirm the total power output through the fiber. The percent transmission fraction was then calculated as the ratio between the power measured through tissue and the power measured through solution. The power intensity was then calculated by considering the light intensity spread due to the conical shape of the 30 mW light output from a 400 μ m fiber based on the fiber's numerical aperture of 0.37 (S5). The fiber output was assumed to be uniform across the diameter of the cone. Measurements were made through grey matter in three blocks of brain tissue for each wavelength with one block each moving anterior-posterior in the thalamus and in the cortex and dorsal-ventral through the thalamus.

Analysis of Electrophysiological Data

Threshold search in Clampfit was used for automated detection of spikes in the multi-unit recording, which was then validated by visual inspection; the spike waveforms displayed by Clampfit were observed to check the quality of spike detection. For traces with multiple spike populations, thresholds were set to capture all the spikes; during bursting, it is likely that multiple neurons were recorded from simultaneously. Bursts were identified in Clampfit; any two consecutive spikes occurring in an interval less than 300 ms were counted as belonging to the same burst and only bursts of at least 3 spikes were included. To quantify the neural activity at different frequencies, spectra for *in vivo* extracellular recording traces were generated using a wavelet transform after converting the traces into binary spike trains. The trace was then converted into a histogram with a binwidth of 0.5 ms for each of the duration-matched pre-stimulation, stimulation, and post-stimulation epochs. The start and end times for each of the segments, as well as the number of spikes, are listed below.

	<i>Pre Stimulation</i>			<i>Light On</i>			<i>Post Stimulation</i>		
	Start	End	Spikes	Start	End	Spikes	Start	End	Spikes
Fig 1 (CaMKIIα::eNpHR)	32.5	72.5	413	102.5	142.5	84	175	215	435
Fig 3 (CaMKIIα::Chr2, HFS)	5.28	10.4	238	15.38	20.5	477	22.48	27.6	235
Fig 5 (Thy1::Chr2,HFS)	0	10.62	90	14.98	25.6	0	29.38	40	94
Fig 5 (Thy1::Chr2, LFS)	0	10.62	139	14.98	25.6	383	29.38	40	132
Fig 6 (Thy1, HFS M1, M1 recd)	0.8	4.8	55	15.46	19.46	28	26	30	30
Fig 6 (Thy1, HFS M1, STN recd)	0.94	5.4	19	15	19.46	37	25.54	30	16
Fig 6 (Thy1, LFS M1, M1 recd)	0	5.5	131	18.5	24	313	30.5	36	64
Fig 6 (Thy1, LFS M1, STN recd)	0	5.5	50	18.5	24	115	30.5	36	39
Fig S4 (eNpHR, small unit)	32.5	72.5	263	102.5	142.5	84	175	215	248
Fig S4 (eNpHR, large unit)	32.5	72.5	114	102.5	142.5	0	175	215	145

Table S1. The three segments of each power spectra were time matched; this table shows the segments of each trace (the start and end time in seconds), as well as the number of spikes detected during each period. Time intervals were chosen to reflect stationary states before, during, and after stimulation for each trace, to account for temporal delays in onset or offset of physiological effects.

The spike histograms were then convolved with a wavelet to measure the amplitude of the spectra at frequencies below 150 Hz over time. The average amplitude over time for each frequency was then plotted. The wavelet used is reproduced below.

$$g(f, t) = e^{-t^2/2\sigma^2} e^{-2\pi i f t}$$

$$\sigma = 4/(3f).$$

For determining the change in activity of multiple frequency bands, amplitude spectra for multiple duration-matched baseline and stimulation sweeps were calculated as described above. Mean amplitude within each frequency band was determined and the ratio of this value (stimulation/baseline) was calculated. Spike latencies of the M1 response to optical stimulation of the STN were determined by measuring the delay between the first peaks in simultaneous optrode recordings of M1 and STN of a Thy1::ChR2-EYFP 6-OHDA mouse. 20 Hz, 5 ms pulse width of 473nm light was used to activate the STN.

SUPPLEMENTARY FIGURES

Fig. S1: Substantia nigra lesion and cannula track. Loss of nigral dopaminergic cells following 6-OHDA administration in rat (A) and mouse (B): coronal slices (rat: AP -5.8; mouse AP -3) show decreased tyrosine hydroxylase levels (red) unilaterally in the substantia nigra pars compacta; SNc is outlined by white brackets. Insets below show higher resolution images of the lesioned (*left*) and unlesioned (*right*) sides of the substantia nigra. (C) Cannula track is visible in a coronal slice showing correct placement of the cannula above the STN area.

Fig. S2: Additional histological characterization. (A) STN cells expressing CaMKII α ::eNpHR-EYFP (green) label for the excitatory neuron specific glutamate marker (red). (B) STN cells expressing GFAP::ChR2-mCherry (red) costain with the astroglia-specific marker S100 β (green). In both (A) and (B) yellow indicates colocalization of the two markers. (C) Representative confocal images of TH stain for dopamine (*top*) and CHAT stain for acetylcholine (*bottom*) showed no colocalization with Thy1::ChR2-EYFP expression in the STN.

Fig. S3: Additional behavioral results. (A) Continuous 473nm illumination of the STN expressing GFAP::ChR2-mCherry in an anesthetized 6-OHDA mouse completely inhibited STN activity. (B) and (C): Extension of mouse results. (B) Amphetamine-induced rotations were not affected by 50% duty cycle illumination of the GFAP::ChR2 expressing STN in 6-OHDA mice (n = 1 mouse and 2 sessions). (C) Amphetamine-induced rotations were not affected by high (130 Hz, 5ms pulse width, n = 1 mouse and 2 sessions) or low (20 Hz, 5ms, n = 1 mouse and 1 session) frequency optical stimulation in the CaMKII α ::ChR2 expressing STN in 6-OHDA mice. (D) and (C): Modulation of inhibitory neurons during behavior. Although mainly excitatory, STN has about 7-10% percent cells that stain for inhibitory neuronal markers, such as GAD65/67 and parvalbumin (Allen Brain Atlas). To obtain specific expression in either GAD67 or parvalbumin neurons we injected GAD67-Cre and parvalbumin-Cre mice respectively (gift of Sylvia Arber) with a Cre-inducible adeno-associated virus (AAV) vector carrying ChR2-EYFP (Methods). Cre-dependent opsin expression was observed in the STN region, but behavior was

unchanged with optical stimulation. (D) Amphetamine-induced rotations were not affected by high (130 Hz, 5ms, n = 2 mice and 4 sessions) or low (20 Hz, 5ms, n = 1 mouse and 2 sessions) frequency optical stimulation in 6-OHDA GAD67-Cre mice. (E) Amphetamine-induced rotations were not affected by high (130 Hz, 5ms, n = 2 mice and 2 sessions) or low (20 Hz, 5ms, n = 2 mice and 2 sessions) frequency optical stimulation in 6-OHDA parvalbumin-Cre mice.

Fig. S4: Additional electrophysiological results. Isolation of large amplitude (A) and small amplitude (B) units from the trace in Fig. 1C and corresponding power spectra. Red lines represent average waveforms for all superimposed spikes that occurred during 70s of baseline activity (n = 205 spikes for large amplitude unit and n = 428 spikes for small amplitude unit). Both small and large amplitude units showed decreased activity during light that returned to normal baseline levels after stimulation. (C) Response of STN to optical stimulation of STN in a Thy1::ChR2-EYFP 6-OHDA mouse at 90Hz. The STN is initially excited but activity is reduced in the emergent stationary state measured by loss of the large amplitude spikes evident during the baseline; nevertheless, significant low amplitude activity persists throughout the stimulation. (D) High-temporal resolution trace of the STN response to optical stimulation of STN in a Thy1::ChR2-EYFP 6-OHDA mouse at 130Hz (see Fig. 5B for full trace). Again, the STN initially responds with a spike followed by low amplitude activity throughout stimulation. Changes in amplitude of the local circuit responses can reflect either altered recruited cell number or altered excitability of recruited cellular elements. While optrode recordings cannot report on the precise cell types involved in generating activity, by eliminating the electrical stimulation artifact these recordings provide a window into the amplitude and timing properties of local circuit electrical responses arising from local excitatory or inhibitory cell types and fibers in the STN region that could not be achieved with electrical stimulation.

Fig. S5: High-temporal resolution optrode traces. (A) Single unit activity in CaMKII α ::eNpHR-EYFP expressing STN with continuous 561 nm light illumination in an anesthetized 6-OHDA rat (corresponding to trace in Fig. 1C). (B) Neuronal activity in CaMKII α ::ChR2-mCherry expressing STN with high frequency optical stimulation (120 Hz, 5 ms pulse width, 473 nm) in an anesthetized 6-OHDA rat (corresponding to trace in Fig. 3B). (C) and (D) Activity in the STN

region in an anesthetized Thy1::ChR2-EYFP 6-OHDA mouse in response to high (HFS, 130 Hz, 5 ms) and low (LFS, 20 Hz, 5 ms) frequency optical stimulation using 473 nm light. Note the low amplitude of activity in the HFS trace (corresponding to trace in Fig. 5B).

Fig. S6: Latency of M1 response to optical stimulation of STN. (A) Response of M1 Layer 5 (L5) to optical stimulation of STN in the Thy1::ChR2-EYFP 6-OHDA mouse at 20Hz, 5ms pulse width. (B) While stimulating STN with light, simultaneous recordings of light-induced activity in the STN (*top trace*) and M1/L5 (*bottom trace*) revealed short latency differences between the first peaks consistent with antidromic spiking. (C) Individual latency differences between the first peak in STN and M1/L5 for 16 stimulation bouts revealed minimal jitter (S.D. = 0.032 ms) consistent with antidromic spiking in the well-known M1-STN projection.

Fig. S7: Changes in frequency characteristics of neuronal activity produced by optical stimulation. (A) Activity in all frequency bands was reduced by continuous 561nm illumination of the STN expressing CaMKII α ::eNpHR-EYFP in anesthetized 6-OHDA rats (n = 5 sweeps). Frequency bands are defined as: delta 1-3 Hz; theta 4-8 Hz; alpha 9-12 Hz; beta 13-30 Hz; gamma 31-80 Hz; high frequency (HF) 81-130 Hz. (B) Optical HFS (120 Hz, 5 ms pulse width) of the STN expressing CaMKII α ::ChR2-mCherry in 6-OHDA rats reduced activity for frequencies between 4 and 80 Hz, while increasing activity in the HF band (n = 3). (C) Activity change in M1 (*left*, n = 4) and STN (*right*, n = 4) produced by optical HFS (130 Hz, 5 ms) stimulation of M1 in 6-OHDA Thy1::ChR2 mice. Delta activity in both M1 and STN was reduced. (D) Activity change in M1 (*left*, n = 4) and STN (*right*, n = 4) produced by optical LFS (20 Hz, 5 ms) stimulation of M1 in 6-OHDA Thy1::ChR2 mice. Beta, gamma, and HF activity in both M1 and STN was increased. (E) Optical LFS (20 Hz, 5 ms) of the STN in 6-OHDA Thy1::ChR2 mice increased activity in the beta, gamma, and HF bands (n = 3). (F) Spike counts for duration-matched baseline and optical stimulation segments for each experiment type. Optical stimulation of the STN expressing CaMKII α ::GFAP-mCherry and optical HFS in 6-OHDA Thy1::ChR2 mice abolished spiking activity, reducing activity across all frequencies to zero (not shown). Error bars are s.e.m.; *t*-test with $\mu = 100$ used for statistics, * $p < 0.05$.

Figure S1

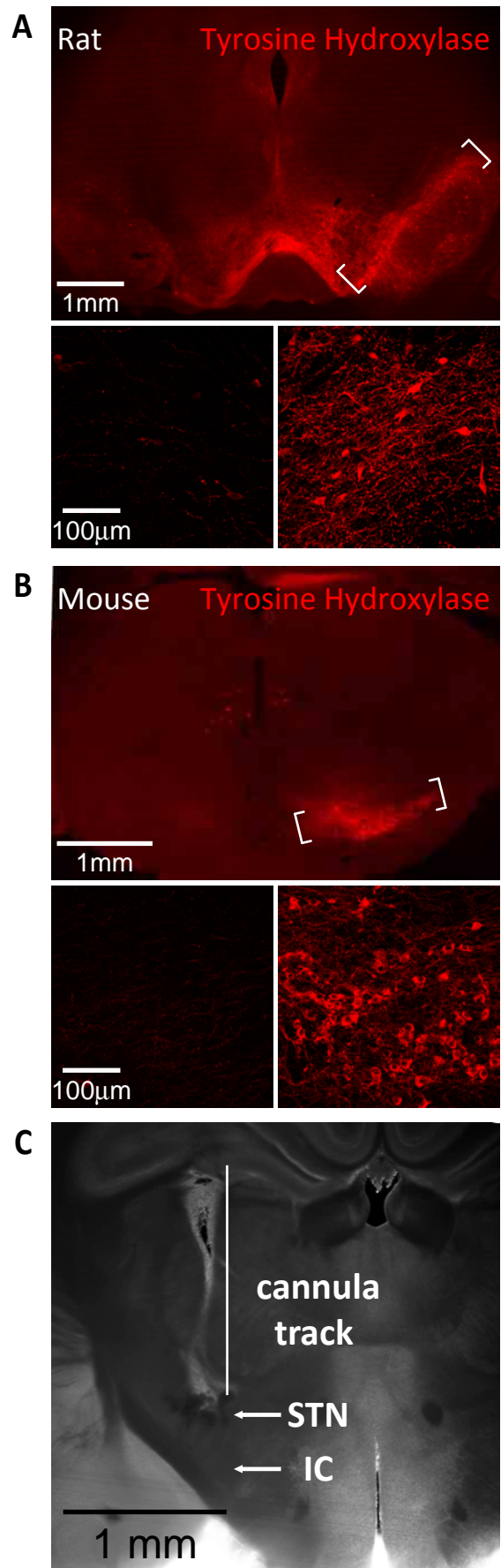


Figure S2

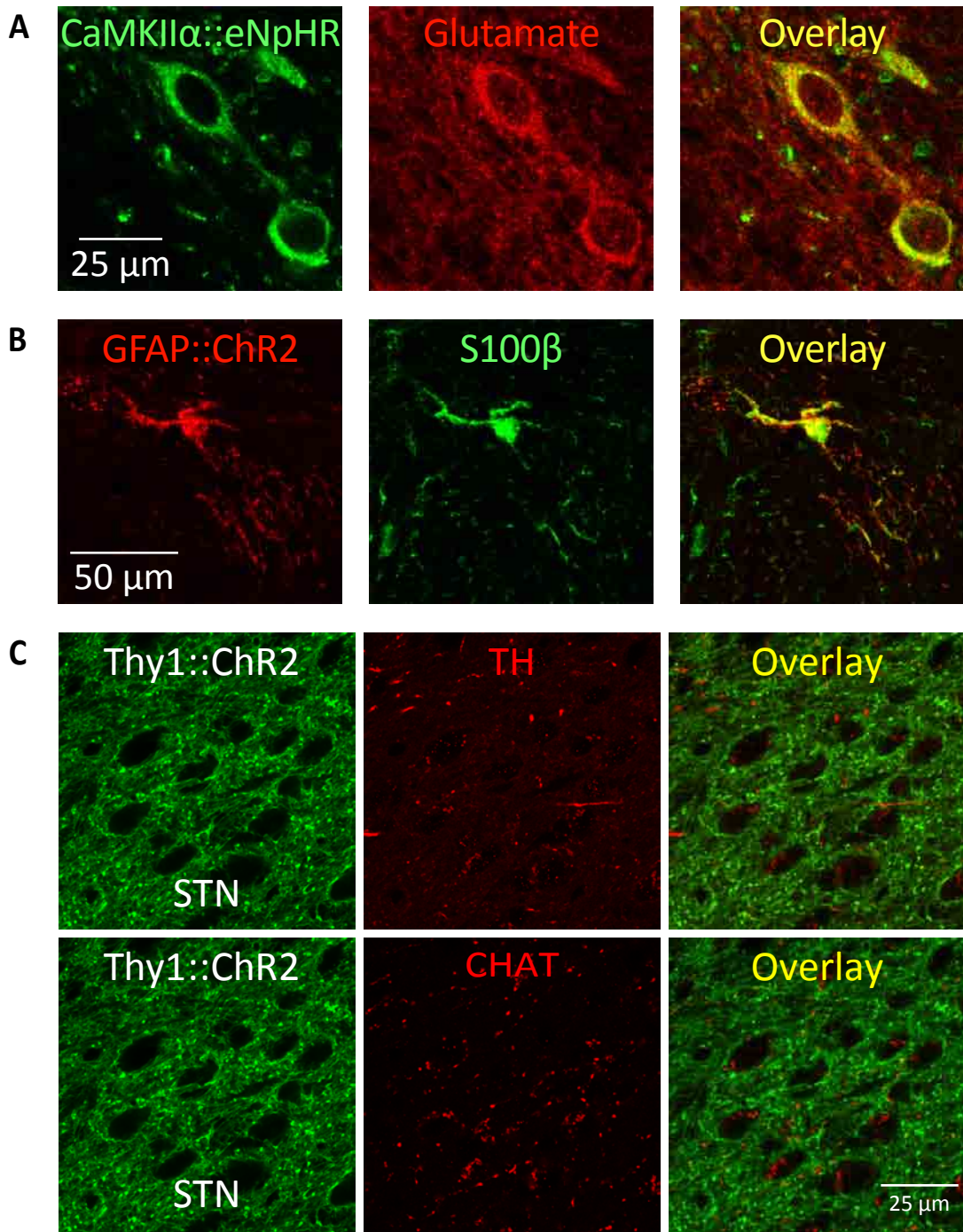


Figure S3

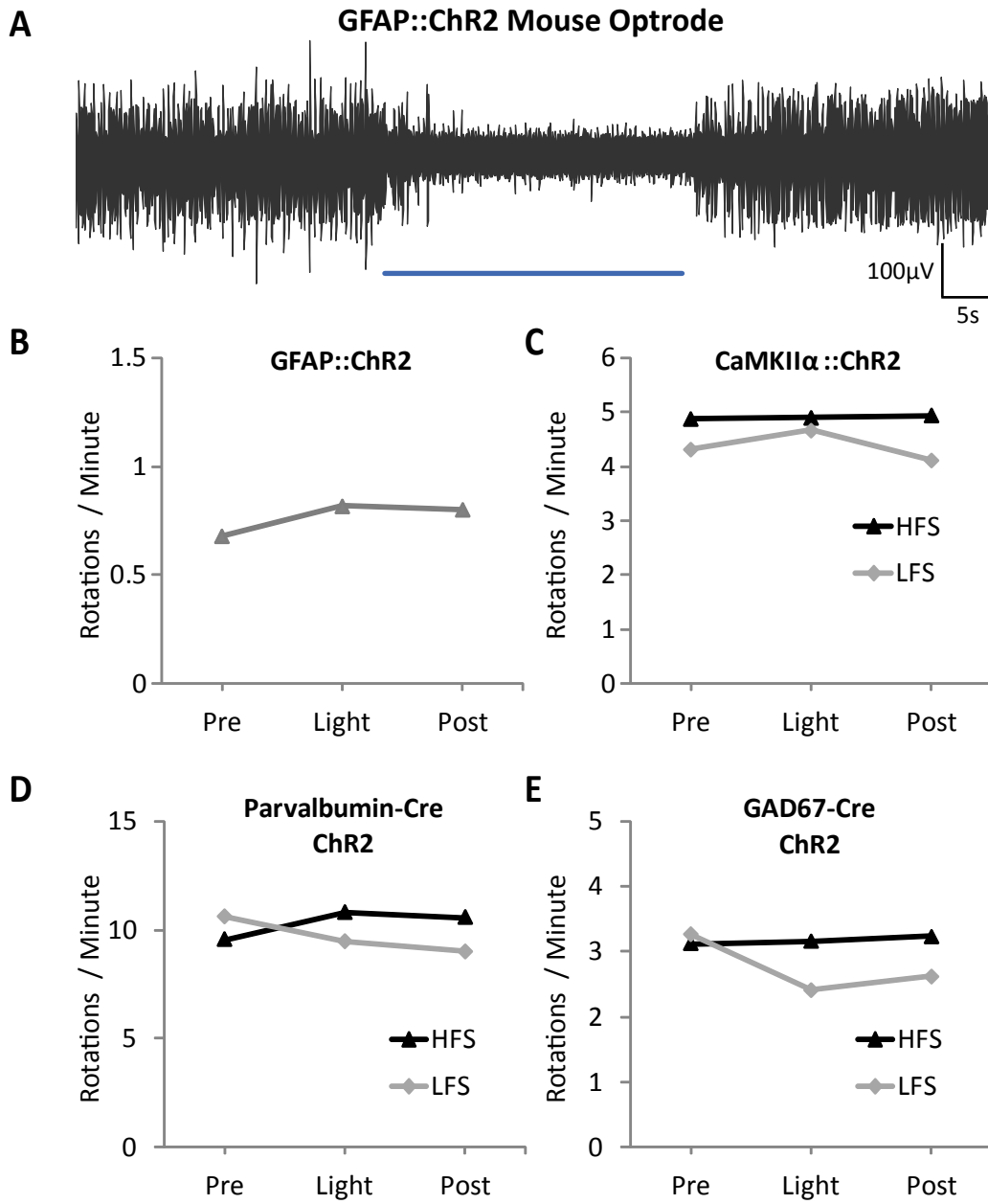


Figure S4

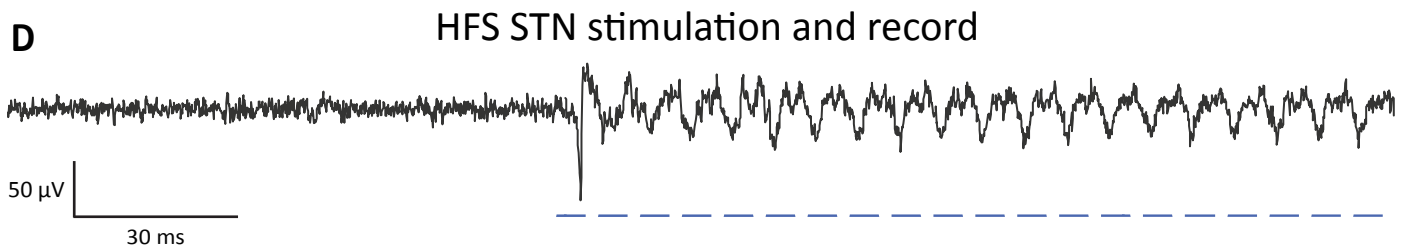
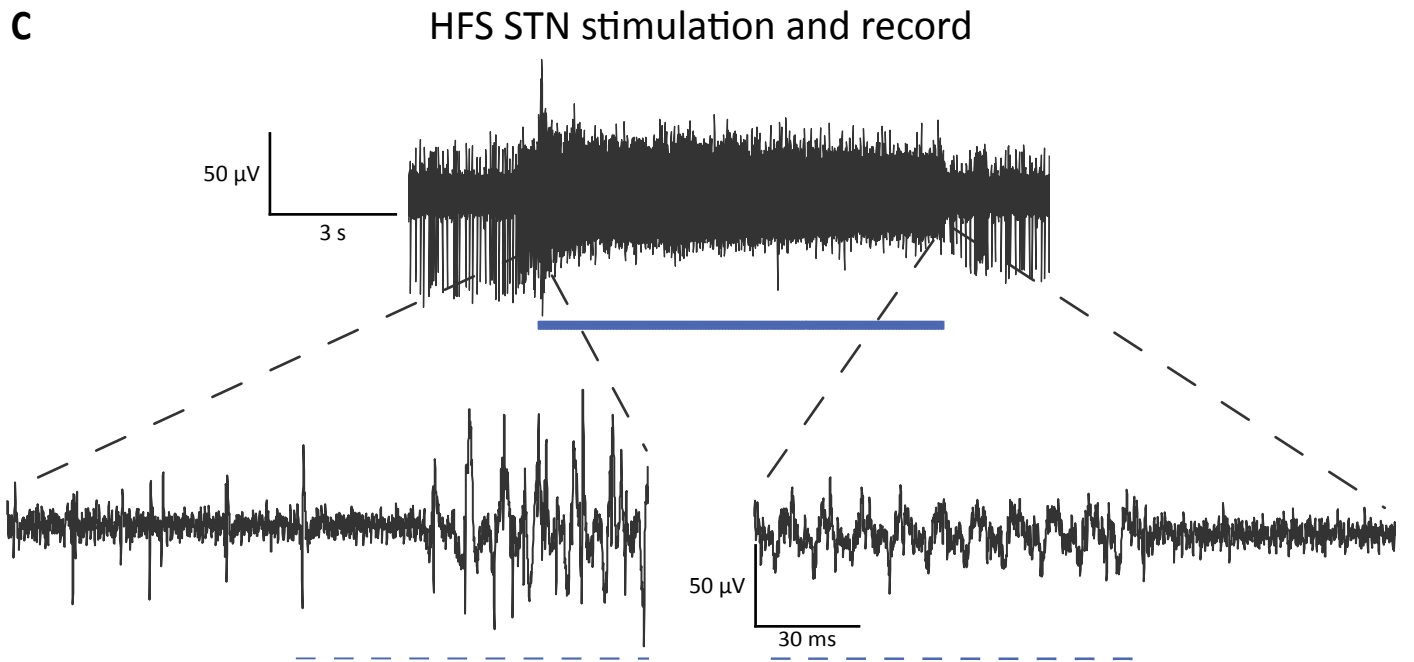
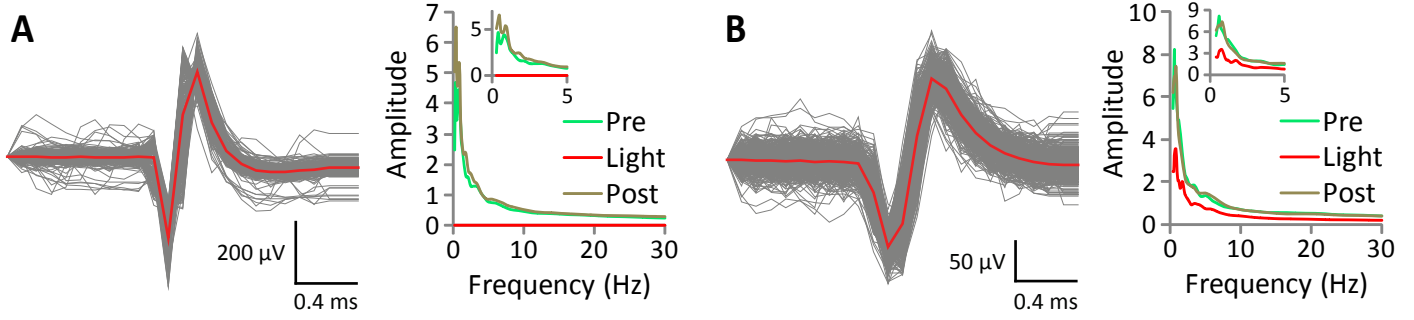
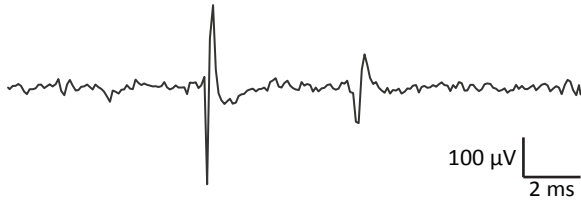


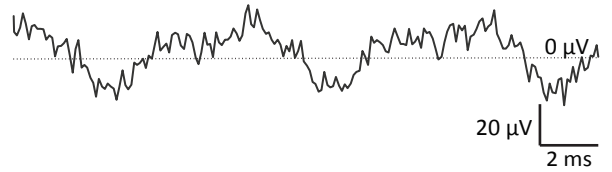
Figure S5

High-Temporal Resolution Traces

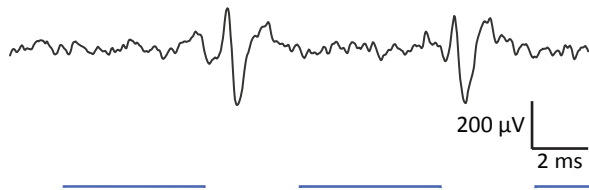
A eNpHR Stimulation in STN (Fig 1C)



C Thy1 HFS Stimulation in STN (Fig 5B)



B Chr2 HFS Stimulation in STN (Fig 3B)



D Thy1 LFS Stimulation in STN (Fig 5B)

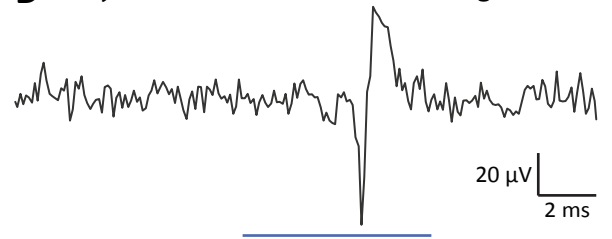


Figure S6

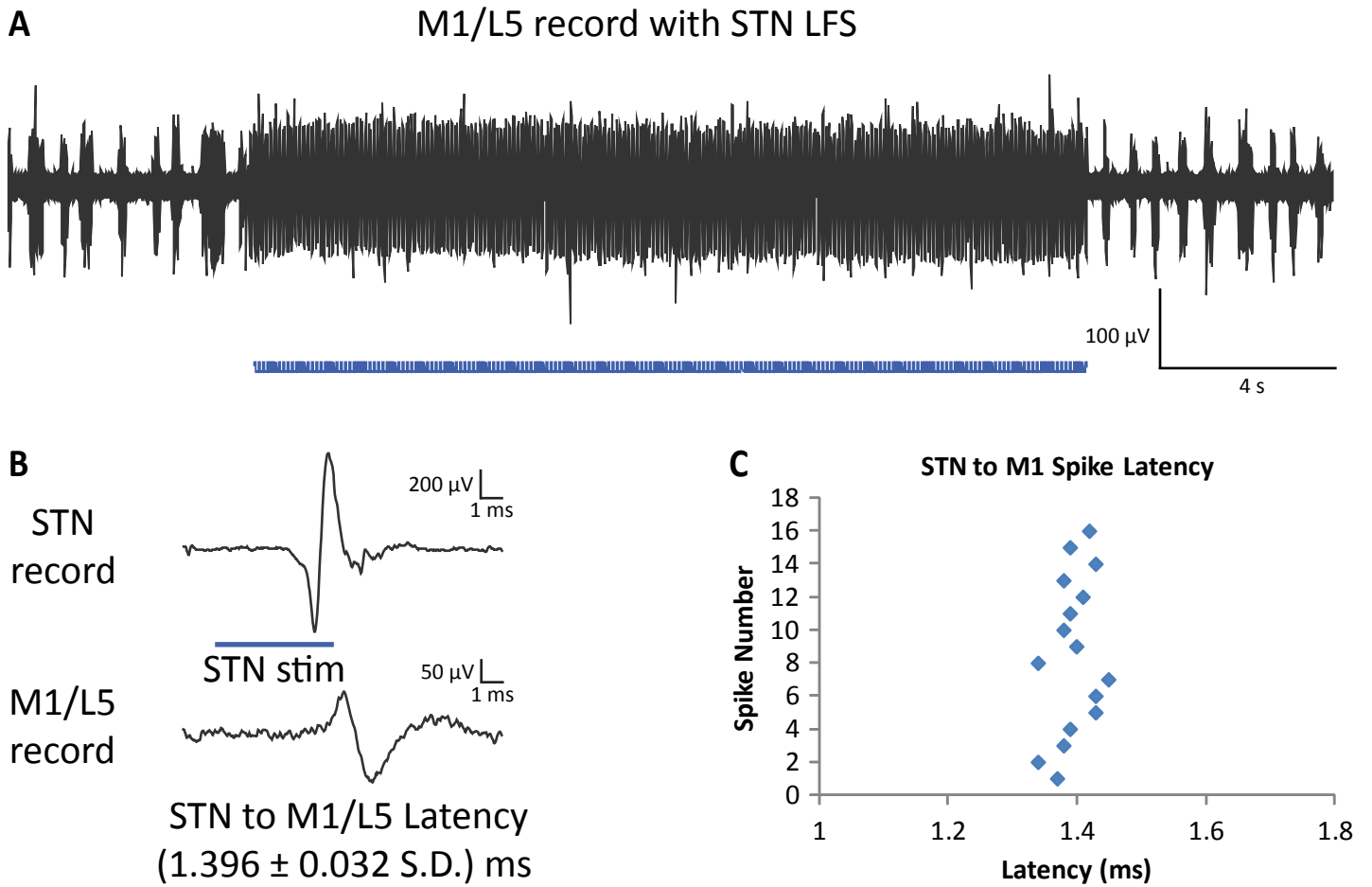
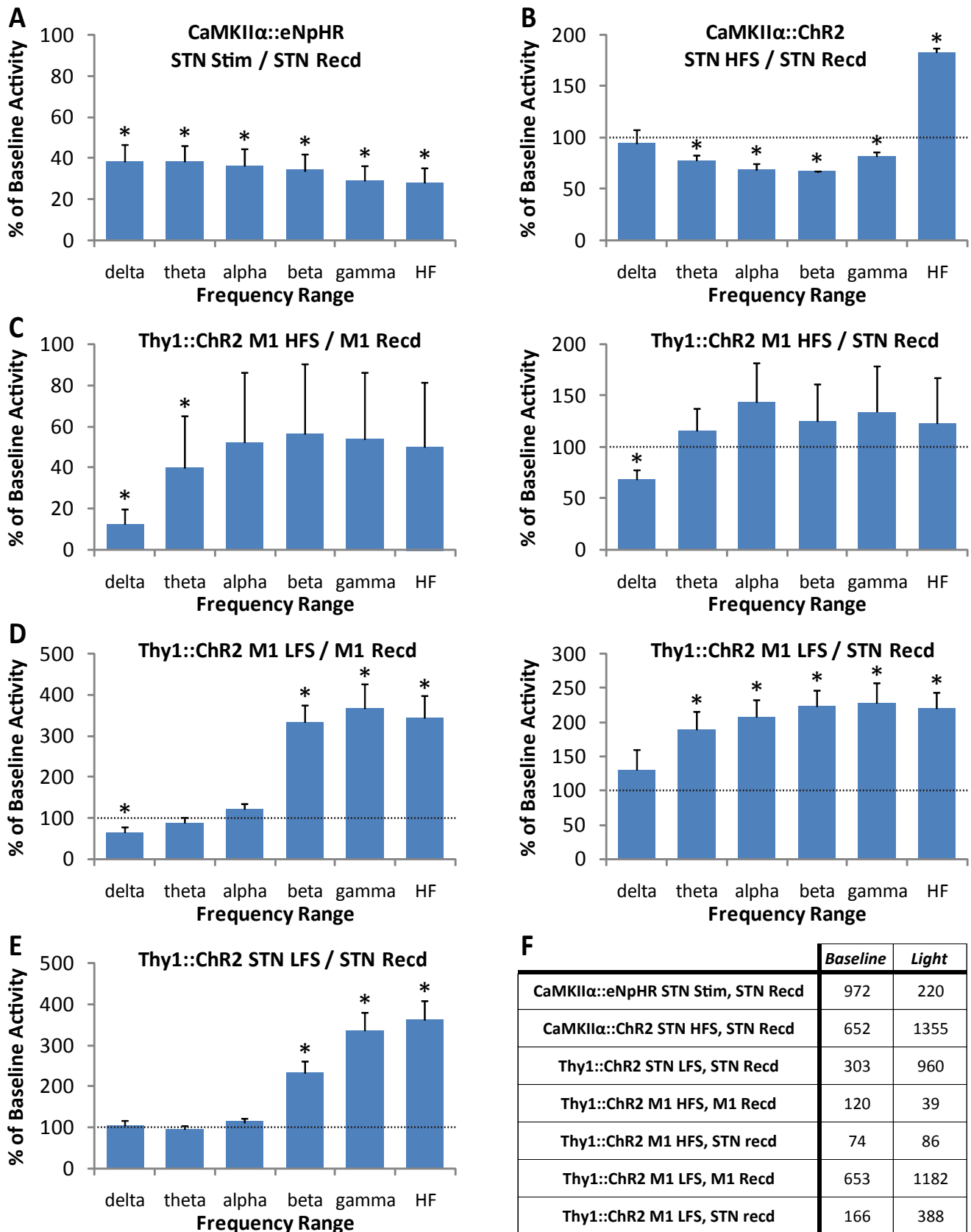


Figure S7



REFERENCES

- S1. V. Gradinaru, K. R. Thompson, K. Deisseroth, *Brain Cell Biol* (Aug 2, 2008).
- S2. F. Zhang *et al.*, *Nature* **446**, 633 (Apr 5, 2007).
- S3. V. Gradinaru *et al.*, *J Neurosci* **27**, 14231 (Dec 26, 2007).
- S4. A. R. Adamantidis, F. Zhang, A. M. Aravanis, K. Deisseroth, L. de Lecea, *Nature* **450**, 420 (Nov 15, 2007).
- S5. A. M. Aravanis *et al.*, *J Neural Eng* **4**, S143 (Sep, 2007).